



Article

Performance Improvement of Innovative Shear Damper Using Diagonal Stiffeners for Concentrically Braced Frame Systems

Chanachai Thongchom ¹, Alireza Bahrami ^{2,*}, Ali Ghamari ³ and Omrane Benjeddou ⁴

¹ Department of Civil Engineering, Faculty of Engineering, Thammasat School of Engineering, Thammasat University, Pathumthani 12120, Thailand

² Department of Building Engineering, Energy Systems, and Sustainability Science, Faculty of Engineering and Sustainable Development, University of Gävle, 801 76 Gävle, Sweden

³ Department of Civil Engineering, Ilam Branch, Islamic Azad University, Ilam, Iran

⁴ Department of Civil Engineering, College of Engineering, Prince Sattam bin Abdulaziz University, Al-Kharj 16273, Saudi Arabia

* Correspondence: alireza.bahrami@hig.se

Abstract: Although concentrically braced frame (CBF) systems enjoy high elastic stiffness and lateral strength, they show a low seismic energy absorption capacity. This dilemma is due to the buckling of CBFs' diagonal members under compressive loading. To overcome the shortcoming, researchers have proposed the use of dampers to improve the behavior of CBF systems. Among the proposed dampers, the metallic shear damper is the most popular thanks to its suitable performance as well as its economic profit. The main shortcoming of the shear dampers is low stiffness. Therefore, in this article, an innovative approach is proposed to improve the behavior of the shear dampers. Subsequently, strengthening the shear damper with X-stiffeners is proposed, and its behavior is evaluated numerically and parametrically. Results indicate that by adding the X-stiffeners, the ultimate strength and elastic stiffness of the shear dampers are enhanced considerably. However, the properties of the stiffeners do not impact the stiffness in the nonlinear zone. Moreover, the behavior of the dampers is affected by parameters such as the ratio of the strength of the web plate to the flange plates, the ratio of the X-stiffeners to the flange plates, and the ρ factor. To consider the parameters to predict the behavior of the damper, required equations are proposed which demonstrate a good agreement with finite element results.

Keywords: shear damper; diagonal stiffener; concentrically braced frame system; strength; stiffness; finite element



Citation: Thongchom, C.; Bahrami, A.; Ghamari, A.; Benjeddou, O. Performance Improvement of Innovative Shear Damper Using Diagonal Stiffeners for Concentrically Braced Frame Systems. *Buildings* **2022**, *12*, 1794. <https://doi.org/10.3390/buildings12111794>

Academic Editor: Enrico Tubaldi

Received: 24 September 2022

Accepted: 21 October 2022

Published: 26 October 2022

Publisher's Note: MDPI stays neutral with regard to jurisdictional claims in published maps and institutional affiliations.



Copyright: © 2022 by the authors. Licensee MDPI, Basel, Switzerland. This article is an open access article distributed under the terms and conditions of the Creative Commons Attribution (CC BY) license (<https://creativecommons.org/licenses/by/4.0/>).

1. Introduction

Among the conventional lateral load-bearing systems, namely concentrically braced frame (CBF), eccentrically braced frame (EBF), and moment resisting frame (MRF), the CBF system has the highest lateral elastic stiffness and ultimate strength but has the lowest ductility [1]. The inherent property of the low ductility of the CBF system is owing to the buckling of the diagonal members of the brace, which causes the system to have low energy dissipation and low ductility. In the inelastic zone, this buckling also degrades lateral stiffness and strength. Because of this important problem, the CBF system is not suitable for high seismic risk zones in spite of its considerable high lateral elastic stiffness and lateral strength.

During the past decades, researchers have been trying to overcome the weakness of CBF systems. To do so, improvement of the CBF systems' behavior utilizing dampers such as metallic dampers [2–4], viscous dampers [5–7], friction dampers [8–10], and buckling-restrained braces (BRBs) [11–14] has been shown to be a successful approach to achieving the aim.

Manufacturing and producing these dampers need special equipment (or high-tech technology) and specialist engineers, which increases the dampers' cost. The increase in construction costs due to the high price of the dampers means that they are not economically justified to be used for conventional structures.

Among the available dampers, metallic dampers are more economical than others, which is achieved through the inelastic deformation of the metallic material [15]. Various metallic dampers have been proposed to enhance the behavior of the CBF systems, including TADAS [16–18], ADAS [19], slit damper [20,21], and shear dampers [22–24]. These devices have mainly been designed to be incorporated into the bracing systems of structural frames. The main feature of the dampers is changing the buckling of the diagonal brace elements of the CBFs so that the dampers yield before other elements.

A comparison of the performance and the economic aspects of metallic dampers illustrates that shear dampers are more popular because they are more economical and easier to construct and install than others [25]. Shear dampers prevent the buckling of the diagonal member of the CBF systems. Therefore, its behavior is enhanced. Although the shear dampers improve the behavior of the CBF systems in terms of ductility and energy dissipation, they reduce the stiffness of the CBF systems [23,25,26]. However, the EBF systems are accounted as shear dampers that have a ductile behavior under seismic loading. The performance of the EBF systems is affected by the performance of the link segment. Comprehensive findings reported in [27–30] clarified that a properly designed shear link can provide a ductile and stable behavior under cyclic loading. Bahrami and Heidari [31,32] investigated the structural response of the EBFs and BRBs having different kinds of links.

The main shortcoming of the EBF systems is the difficulty of replacing the link after a severe earthquake because the link is a part of the floor beam, and if the floor beam also carries the gravity load, the costs and problems of replacing the link beam will be much higher. In some cases, repairing the brace may not be economically acceptable. To overcome these disadvantages, the EBF systems were developed by Seki et al. [33] as an efficient lateral load-resisting system using the vertical shear link as V-EBF systems. In V-EBFs, a shear link is attached between the floor beam and chevron brace. The use of the V-EBF systems instead of the conventional EBFs was recommended in [34–36] to improve the ability of replacement after severe earthquakes. The main flaw of the V-EBF systems is their lower elastic stiffness and higher construction cost compared with conventional EBF systems [37].

Generally, the mentioned dampers, such as metallic dampers, viscous dampers, and friction dampers, and also shear links (EBFs, V-EBFs, and shear dampers) are installed between the chevron brace and floor beam; however, they can be attached directly to the diagonal brace elements. Installing the damper between the chevron CBF and floor beam causes difficulty in construction because it needs additional gusset plates. Moreover, they impose high force on the floor beam. Accordingly, for these systems, a beam with a high moment of inertia is required. Due to transferring stresses from the damper to the floor beam, the floor beam may experience nonlinear behavior. For these situations, replacing the damper and floor beam after earthquakes is complicated, especially when the floor beam carries the gravity loads. Although directly installing dampers on the diagonal members of the CBFs solves this problem and improves the behavior of the CBFs, as mentioned before, they reduce the elastic stiffness and ultimate strength of the CBFs. To overcome this shortcoming, in the current article, an innovative shear damper (I-shaped damper diagonally stiffened with X-stiffeners) is introduced and studied numerically and parametrically. The main feature of this damper is to improve the stiffness and strength of the I-shaped shear damper. The proposed damper is also detailed in such a way that it would not be complicated to construct and install. The advantages of the system, such as simplicity in construction, low cost of preparing the damper, and easy replacement after an earthquake, justify the damper from an economic point of view. Furthermore, the required equations for the design of the damper are driven and presented.

2. Proposed Damper

The proposed damper consists of five plates: shear plate, flange plate, X-stiffeners, middle plate, and boundary plates. Figure 1 displays the schematic view and details of the proposed damper. The middle plate and boundary plates do not contribute to resisting the applied load. It is expected that the shear plate, flange plate, and X-stiffeners share the shear strength. It is observed from Figure 1 that the damper is simple to construct and install. Because this damper can be made outside the building site under strict supervision and then installed on the site, it can eliminate overhead welds and reduce construction and implementation times. These advantages make the damper cost-effective; its construction and installation do not impose much cost on the building. In addition, it enjoys easy replacement after a severe earthquake. Confining the yielding in the proposed damper causes limited damage, and the element outside the damper remains elastic. The remaining structural elements outside the damper reduce repair costs after a severe earthquake, which can be acknowledged as an important factor in justifying the economical nature of this damper.

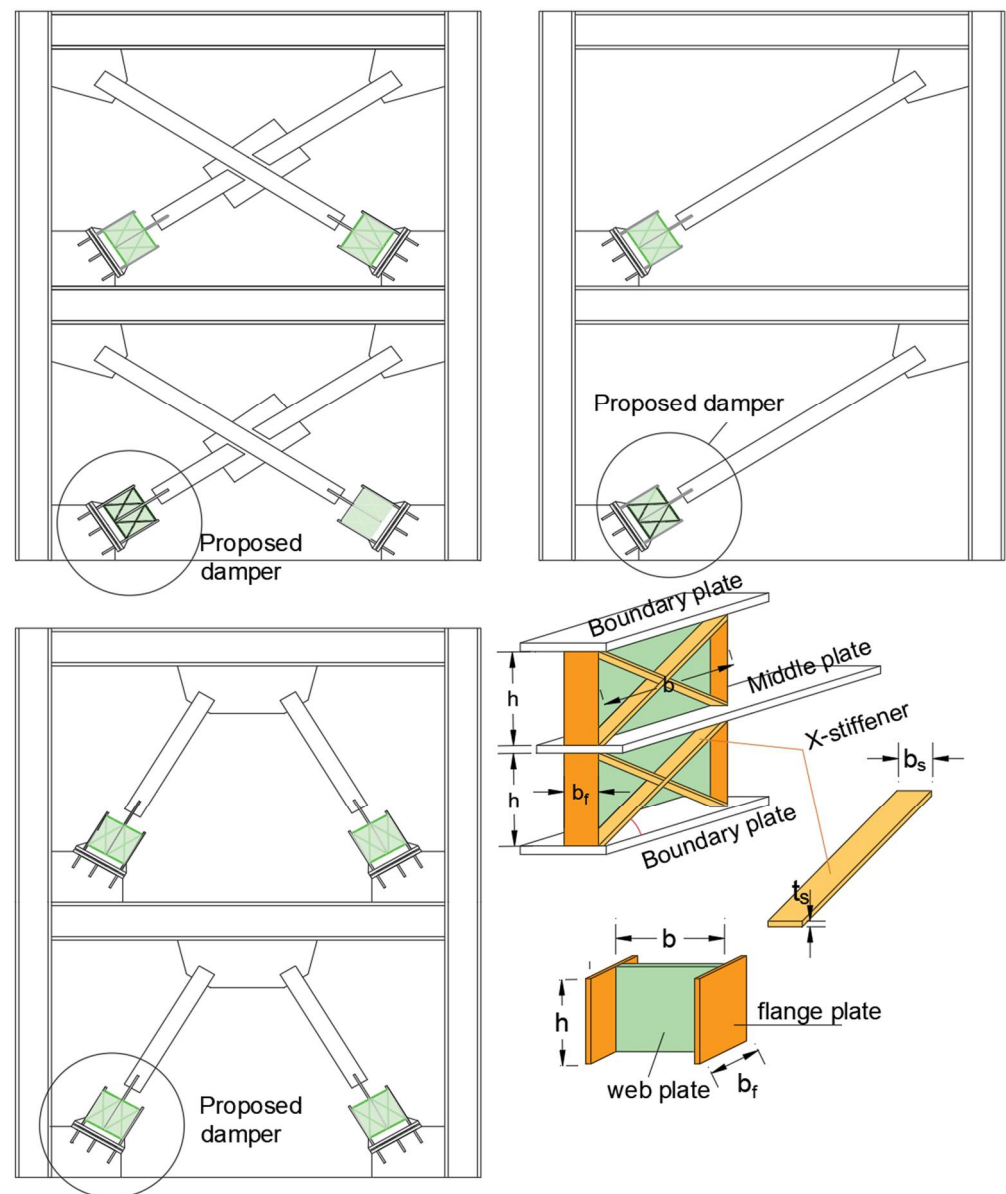


Figure 1. Schematic view and details of proposed damper.

3. Design of Proposed Damper

3.1. Mechanism of Damper

To design the proposed damper, it is expected that hinges will be formed, as illustrated in Figure 2, in the shear plate, flange plate, and X-stiffeners. The derived equations are based on the assumption that their accuracy is examined using finite element (FE) results in the next section.

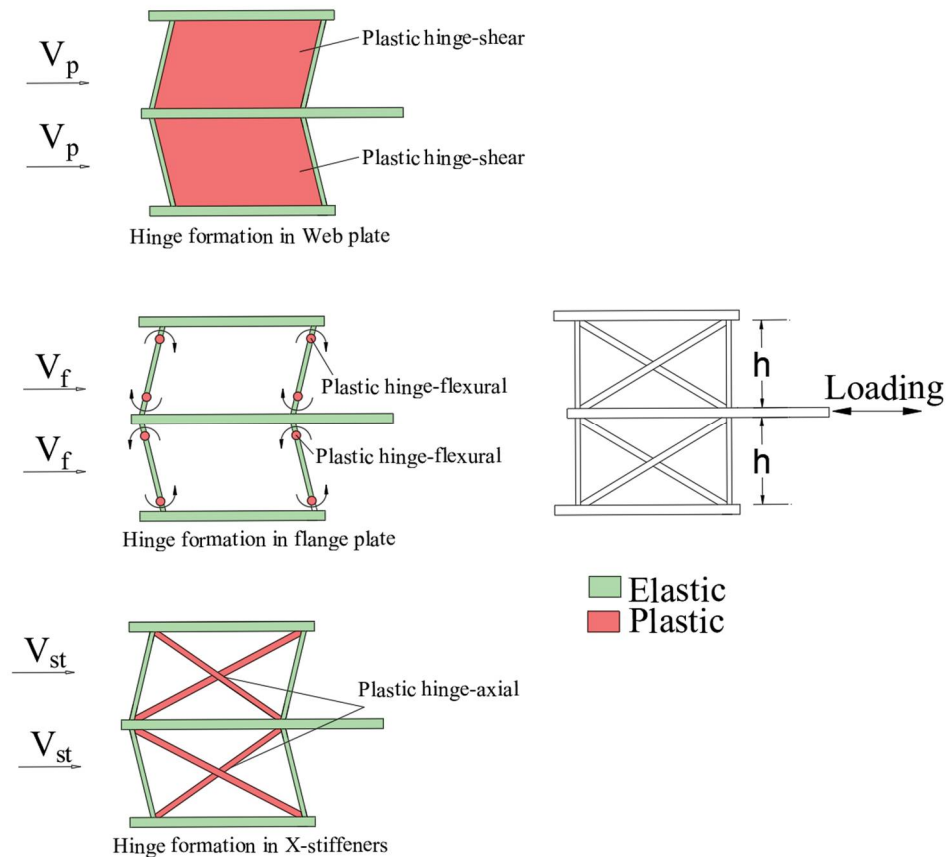


Figure 2. Expected hinge formation over proposed damper.

3.2. Ultimate Strength

According to AISC [38] regarding I-shaped shear links ($\rho < 1.6$), the ultimate strength is determined by $V_p = 0.6F_{yw}bt_p$ where F_{yw} , b , and t_p are yielding stress of the web plate, length of the web plate that is equal to e for the proposed damper, and the web plate thickness, respectively. In this equation, although the shear strength of the flange plate or the load carried by the flange plate is ignored, researchers confirmed in [39–41] that the flanges of I-shaped shear links increase the ultimate shear strength of the shear links. Thus, in this article, it is assumed that the web plate, flange plate, and stiffeners transfer the applied load to the damper. Therefore, the shear strength (nominal shear capacity) of the damper is proposed as:

$$V_n = n(V_p + V_f + V_{st}) \quad (1)$$

where n is the number of the web plates, and V_f and V_{st} represent the shear strength of the flange plate and X-stiffeners, respectively. Additionally, V_p is the shear strength of the web plate which is equal to the plastic shear strength and is calculated using the following equation:

$$V_p = 0.6F_{yw}b't_w \quad (2)$$

In computing V_p , the shear capacity of the flange plates is not ignored. For this reason, the thickness of the flange plates is added to the length of the web plate, which gives $b' = b + 2t_f$.

Equation (1) can be rewritten as follows in which the factors β and β' are defined as $\beta = \frac{V_f}{V_p}$ and $\beta' = \frac{V_s}{V_p}$

$$V_n = nV_p(1 + \beta + \beta') \quad (3)$$

Based on [23,24], it is assumed that the ultimate strength of the flange plate using the plastic theory is given when the flexural hinges are formed at the two ends of the flange plates. Therefore, V_f is obtained as $V_f = \frac{4M_{pf}}{h'}$ where M_{pf} is the plastic moment of the flange plate. Knowing $M_{pf} = \frac{b_f t_f^2}{4} F_{yf}$, V_f is achieved as:

$$V_f = \frac{b_f t_f^2}{h'} F_{yf} \quad (4)$$

where F_{yf} and h are the yielding stress and height of the flange plate, respectively. It is assumed that the length of the plastic hinge on the two ends of the flange plates is about 10% of h of the flange plate. Accordingly, the distance between the plastic joints is equal to $h' = 0.8h$.

3.3. Elastic Stiffness

In accordance with the theory of analysis, the equivalent spring of stiffness acts as parallel springs. Hence, Equation (5) is proposed to calculate the stiffness, K , of the proposed damper:

$$K = n(K_p + K_f + K_s) \quad (5)$$

To show that the stiffeners, as well as the ultimate strength, are affected by β and β' , Equation (5) can be written in the form of:

$$K = nK_p \left(1 + \frac{\Delta_p}{\Delta_f} \beta + \frac{\Delta_p}{\Delta_s} \beta' \right) \quad (6)$$

where K_p , K_f , and K_s are, respectively, the stiffness of the shear plate, flange plate, and X-stiffeners. To determine K_p , it is assumed to be a shear plate under pure shear, where its stiffness is calculated as $K_p = \frac{V_p}{\Delta_p}$. Δ_p is calculated using Equation (7).

$$\Delta_p = \left(\frac{\tau_{cr}}{G} + \frac{2\sigma_{ty}}{E \sin 2\alpha} \right) h \quad (7)$$

In this equation, G is the shear modulus and E is the Young's modulus. Using $E = 2(1 + \nu)G$ and the Poisson's ratio $\nu = 0.3$ for steel, the stiffness is determined as $\Delta_p = \frac{2h}{E} \left(\tau_{cr} + \frac{\sigma_{ty}}{\sin 2\alpha} \right)$. Then, K_p is calculated as:

$$K_p = \frac{0.3Et_p b F_{yp}}{h \left(\tau_{cr} + \frac{\sigma_{ty}}{\sin 2\alpha} \right)} \quad (8)$$

It was assumed that the field action in the shear plate is formed along the X-stiffeners. Thus, its angle is assumed to be α . In addition, σ_{ty} is defined as the equivalent stress that is calculated using [42]:

$$\sigma_{ty} = \frac{-1.5\tau_{cr} \sin 2\alpha \pm \sqrt{(1.5\tau_{cr} \sin 2\alpha)^2 - 2(\sin^4 \alpha + 0.75 \sin^2 2\alpha)(3\tau_{cr}^2 - F_y^2)}}{(\sin^4 \alpha + 0.75 \sin^2 2\alpha)} \quad (9)$$

In this equation, based on the stability theory of plates, the buckling capacity of the shear plate is determined as $\tau_{cr} = \sqrt{K_v \frac{0.4F_y E}{(b/t)^2}} \leq \frac{F_{yw}}{\sqrt{3}}$ where the coefficient K_v is obtained using Equation (10):

$$\begin{cases} K_v = 5.34 + 4(b/h)^2 & \frac{b}{h} \geq 1 \\ K_v = 4 + 5.34(b/h)^2 & \frac{b}{h} \leq 1 \end{cases} \quad (10)$$

Referring to Figure 2, the stiffness of the flange plate is determined as:

$$K_f = \frac{24EI_f}{h^3} \quad (11)$$

where I_f is the moment of inertia of each flange plate.

Moreover, the X-stiffeners act as a truss where their two ends have been joined to the boundary flange plates using pin connection. According to the principal theory of analysis, its stiffness is calculated as:

$$K_s = 2 \frac{EA}{L} \cos^2 \alpha \quad (12)$$

where L is the diagonal length of the X-stiffeners and coefficient 0.75 is applied to L , and A is the sectional area of the X-stiffeners that equals $A = b_s t_s$. This equation can be simplified as $K_s = Eb_s t_s \frac{L}{L^2 + h^2}$.

3.4. Design of Elements outside Damper

To assure the action of the proposed damper as a ductile fuse, this damper should yield before other elements. Therefore, it is recommended to design the element outside the damper by the simplified coefficient as follows:

$$V_{design} = \max(\Omega, 1.25R_y) V_n$$

where V_n is obtained by Equation (3) and Ω is the overstrength of the damper. Ω is determined as the nominal strength, V_n , divided by the strength corresponding to the first hinge formation, V_s .

$$\Omega = \frac{V_n}{V_s} \quad (13)$$

Since at the beginning of the hinge formation, all components are involved, V_s is calculated as:

$$V_s = V_p + \Delta_p K_f + \Delta_p K_s \quad (14)$$

By knowing $\Delta_p = \frac{V_p}{K_p}$, the equation can be simplified as:

$$V_s = V_p \left(1 + \frac{K_f + K_s}{K_p} \right) \quad (15)$$

Finally, Ω can be calculated as:

$$\Omega = \frac{1 + \frac{V_s}{V_p} + \frac{V_f}{V_p}}{1 + \frac{K_f + K_s}{K_p}} \quad (16)$$

This equation confirmed that Ω is obtained greater than 1. With introducing the parameters $\beta = \frac{1}{\psi}$ (where $\psi = \frac{V_f}{V_p}$) and $\beta' = \frac{1}{\psi'}$ (where $\psi' = \frac{V_s}{V_p}$), the overstrength is simplified as $\Omega = \frac{1 + \psi' + \psi}{1 + K_f \frac{\beta}{\beta'} + K_s \frac{\beta'}{\beta}}$.

To assure the suitable performance of the proposed damper, no local buckling must be permitted. As a consequence, L_s/t_s and b_s/t_s should be limited. The optimum value of the ratios is suggested in the next sections according to the FE findings.

4. Parametric Study

In the investigation of the behavior of the proposed damper, some variables are expected to affect the behavior of the damper according to the proposed equations. Therefore, some variables are defined in this study.

Numerical models, including $\beta' = 0.15$ to 1.21, are designed and evaluated. To do so, first, a model with $\beta' = 0.15$ is designed, then it is increased two times as $\beta' = 0.15, 0.30, 0.6$, and 1.21. The main purpose of defining this model is to cover models with $\beta' < 1$ and $\beta' > 1$ with respectively $\Psi' < 1$ and $\Psi' > 1$, meaning that the shear strength of the web plate is respectively lower and larger than the strength of the X-stiffeners. In addition, numerical models including $\Psi = 0.73$ to 5.54 are designed. To achieve this, the thickness of the web plate, t_p , is considered constant (6 mm), and the thickness of the flange plate, t_f , is increased. Like β' , the main aim of introducing β is to be lower and greater than 1. For $\beta < 1$, the strength of the web plate is lower than the strength of the flange plate, whereas, for $\beta > 1$, it is the opposite.

According to AISC [38], the parameter $\rho = e/(M_p/V_p)$ is measured as a key parameter to categorize the behavior of the shear links into the mechanisms of shear ($\rho < 1.6$), shear-flexural ($1.6 < \rho < 2.6$), and flexural ($\rho > 2.6$). In ρ , M_p is the plastic moment, and V_p is the plastic shear capacity of the link, and e is the link length. e is known as a key parameter, while by its reduction, the mechanism tends to have shear behavior.

Since, according to AISC [38], shear links with $\rho < 1.6$ expect to have a shear mechanism, models with different ρ equal to 0.25, 0.18, 0.13, and 0.11 are evaluated. These models are accounted as very short links. Although all the models are with $\rho < 1.6$, unlike the suggestion of AISC [38], it is expected that ρ affects the behavior of the shear links (the proposed damper).

5. Numerical Simulation

5.1. Numerical Models

For the simulation of the numerical models in this study, the FE method was utilized by the ANSYS software. All the components were simulated using SHELL181 elements that are capable of accounting for buckling, nonlinearity, and large displacement. During the analysis, nonlinearities regarding both the materials and geometry were considered.

To investigate the behavior of the damper, the numerical models were designed according to the goals of the parametric study. Consequently, the numerical models are listed in Table 1. In all the models, $h = 140$ mm, $t_p = 6$ mm, and $b_s = b_f = 160$ mm were selected. In this table, a designation was considered for each model. The designation of each damper consists of four parts. The first part represents the type of damper; I for the I-shaped dampers and X for the dampers with X-stiffeners. The second part stands for ρ . The third part introduces β , and the fourth part represents β' . Since the I-shaped dampers do not have β' , N (not applicable) was used for them.

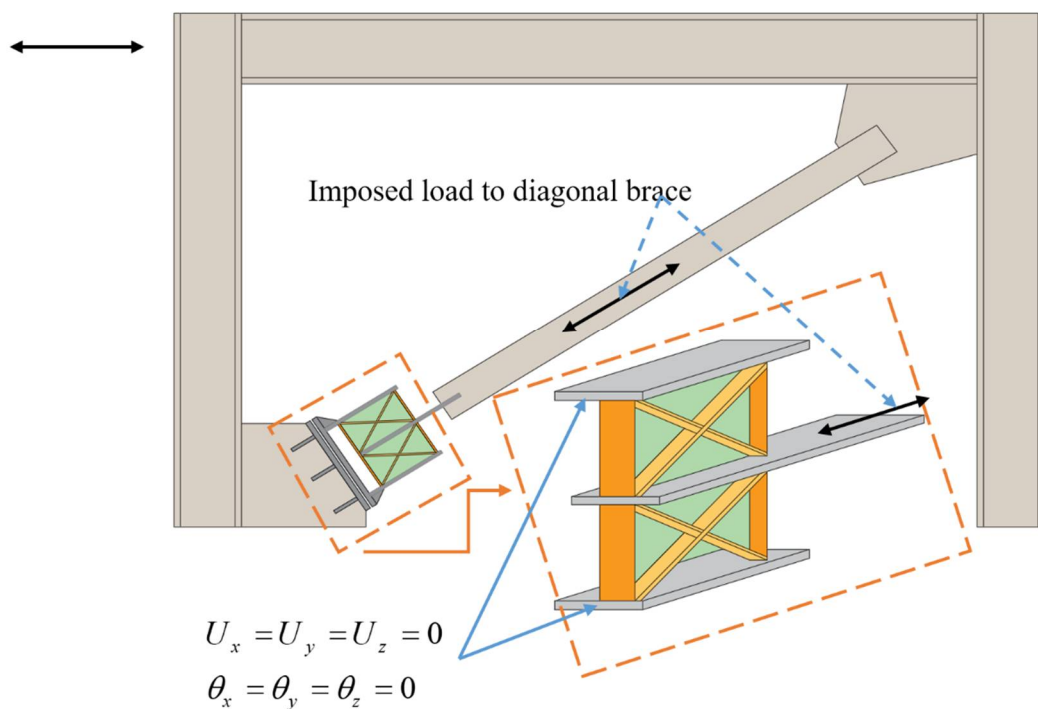
5.2. Boundary Conditions and Materials

To study the proposed damper, the bare damper was analyzed as a simplified damper, demonstrated in Figure 3. Since the beam to columns is connected using pin connection, the main frame does not affect the behavior of the damper. Therefore, the main frame is not simulated. In addition, since this study deals with determining the performance of the proposed damper and examining the accuracy of the proposed relations, only the bare damper is considered. In a future study, the interaction between the damper and the diagonally braced frame will be considered.

Table 1. Properties of numerical models.

| | Model | t_f (mm) | ρ | β | t_s (mm) | β' | β/β' |
|--|------------------|------------|--------|---------|------------|----------|----------------|
| I-shaped dampers | I-0.25-5.54-N | 10 | 0.25 | 5.54 | — | — | — |
| | I-0.18-2.58-N | 15 | 0.18 | 2.58 | — | — | — |
| | I-0.13-1.51-N | 20 | 0.13 | 1.51 | — | — | — |
| | I-0.11-1.01-N | 25 | 0.11 | 1.01 | — | — | — |
| | I-0.09-0.73-N | 30 | 0.09 | 0.73 | — | — | — |
| Dampers strengthened with X-stiffeners | X-0.25-5.54-1.21 | 10 | 0.25 | 5.54 | 2.5 | 1.21 | 4.59 |
| | X-0.25-5.54-0.60 | 10 | 0.25 | 5.54 | 5 | 0.60 | 9.18 |
| | X-0.25-5.54-0.30 | 10 | 0.25 | 5.54 | 10 | 0.30 | 18.35 |
| | X-0.25-5.54-0.15 | 10 | 0.25 | 5.54 | 20 | 0.15 | 36.70 |
| | X-0.18-2.58-1.21 | 15 | 0.18 | 2.58 | 2.5 | 1.21 | 2.04 |
| | X-0.18-2.58-0.60 | 15 | 0.18 | 2.58 | 5 | 0.60 | 4.08 |
| | X-0.18-2.58-0.30 | 15 | 0.18 | 2.58 | 10 | 0.30 | 8.16 |
| | X-0.18-2.58-0.15 | 15 | 0.18 | 2.58 | 20 | 0.15 | 16.31 |
| | X-0.13-1.51-1.21 | 20 | 0.13 | 1.51 | 2.5 | 1.21 | 1.15 |
| | X-0.13-1.51-0.60 | 20 | 0.13 | 1.51 | 5 | 0.60 | 2.29 |
| | X-0.13-1.51-0.30 | 20 | 0.13 | 1.51 | 10 | 0.30 | 4.59 |
| | X-0.13-1.51-0.15 | 20 | 0.13 | 1.51 | 20 | 0.15 | 9.18 |
| | X-0.11-1.01-1.21 | 25 | 0.11 | 1.01 | 2.5 | 1.21 | 0.73 |
| | X-0.11-1.01-0.60 | 25 | 0.11 | 1.01 | 5 | 0.60 | 1.47 |
| | X-0.11-1.01-0.30 | 25 | 0.11 | 1.01 | 10 | 0.30 | 2.94 |
| | X-0.11-1.01-0.15 | 25 | 0.11 | 1.01 | 20 | 0.15 | 5.87 |
| | X-0.09-0.73-1.21 | 30 | 0.09 | 0.73 | 2.5 | 1.21 | 0.51 |
| | X-0.09-0.73-0.60 | 30 | 0.09 | 0.73 | 5 | 0.60 | 1.02 |
| | X-0.09-0.73-0.30 | 30 | 0.09 | 0.73 | 10 | 0.30 | 2.04 |
| | X-0.09-0.73-0.15 | 30 | 0.09 | 0.73 | 20 | 0.15 | 4.08 |

Lateral loading

**Figure 3.** Boundary conditions of simplified damper.

Additionally, A36 steel with a yield strength of 235 MPa, Young's modulus of 200 GPa, and Poisson's ratio of 0.3 were employed for all the components.

5.3. Verification of FE Results

For verification of the FE results of this study, the result of an experimental test reported in [42] is compared with the FE result. The laboratory model consists of an I-shaped shear damper with a height of 80 mm for each web plate and a thickness of 2 mm for the web and flange plates.

In the experimental test, plates with a thickness of 25 mm were selected for the top and middle plates. Furthermore, 6-mm plates were connected to the top and bottom of the main web and flange plates. All the elements were created with A36 steel material.

Figure 4 clarifies that there is a good agreement between the FE result and experimental test result. As shown in the figure, the damper carries the applied loading without degradation up to 7 mm (rotation of 8.5%), which is considerable. Moreover, no fracture occurred in the damper up to 14 mm displacement (rotation of 14.5%), which is an important feature, as high rotation capacity without failure.

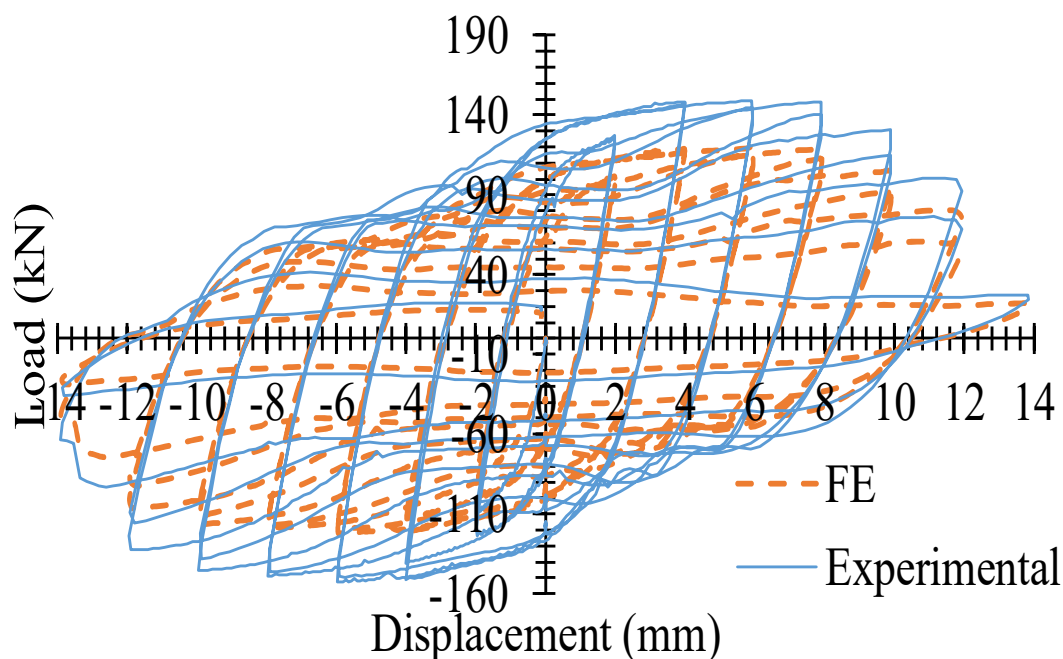


Figure 4. Comparing FE result with experimental test result.

6. Results and Discussion

6.1. Comparing Dampers with and without X-Stiffeners

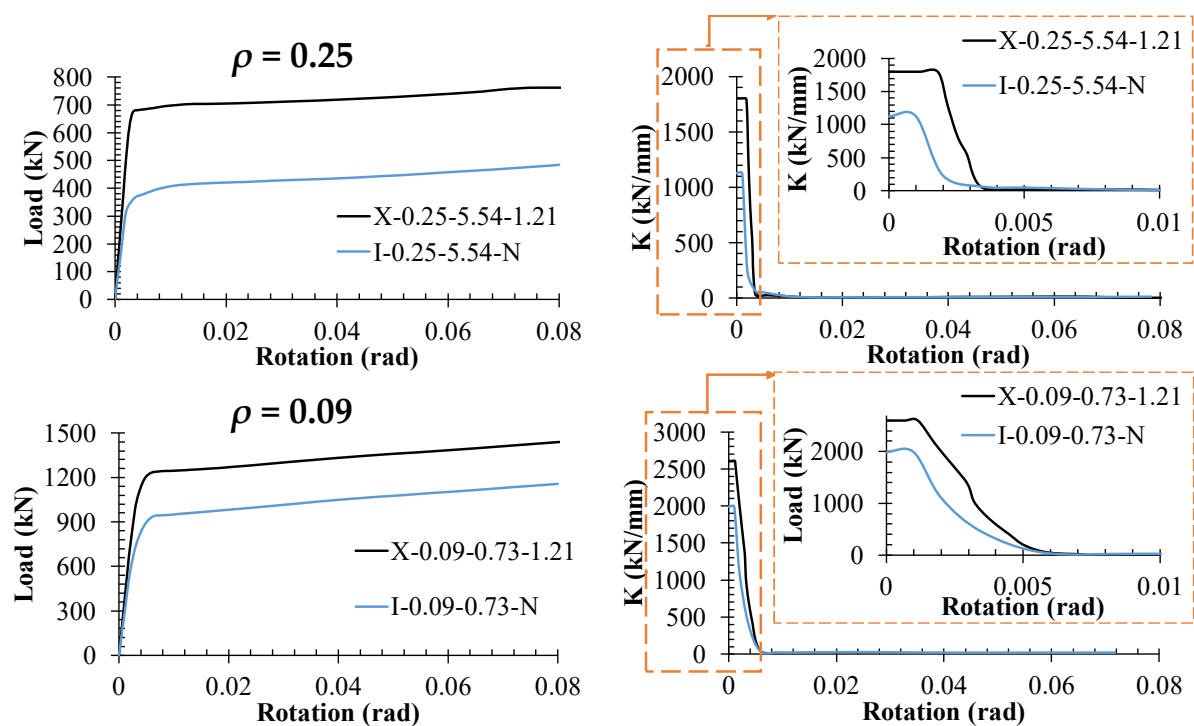
To consider the effect of the diagonal stiffeners on the behavior of the I-shaped damper, their load-rotation and stiffness-rotation graphs were achieved. Figure 5 illustrates the typical graphs for the dampers with $\rho = 0.25$ and $\rho = 0.09$. According to the figure, the diagonal stiffeners improved the behavior of the I-shaped dampers in linear and nonlinear zones. However, there is not a considerable effect on the stiffness at rotation over 0.005. The obtained results of the damper with and without stiffeners are compared in Table 2.

Based on the table, low t_s (thin stiffeners) improve the ultimate strength (F_u) between 19 and 54%, whereas it can be reached 3.5–6.94 times. On the other hand, by adding the stiffeners, F_u is enhanced 1.19–6.94 times depending on the properties of the stiffeners and dampers. Meanwhile, the elastic stiffness is improved by the thin and thick stiffeners, respectively, between 31–60% and 2.89–4.48 times. This value for V_s is measured between 20–74% for the thin stiffeners and 2.89–4.48 times for the thick stiffeners. It is confirmed that the thin stiffeners have the most effect, respectively, on K , V_s , and F_u , while the thick stiffeners have the most influence, respectively, on F_u , V_s , and K .

By adding the thin stiffeners, Ω is reduced around 10%, whereas by increasing t_s , it is improved between 21 and 55%.

Table 2. Comparing results of damper with and without stiffeners.

| Model | t_f (mm) | t_s (mm) | ρ | β | F_u (kN) | K (kN/mm) | V_s | Ω | Stiffened Damper | | | |
|------------------|------------|------------|--------|---------|------------|-------------|--------|----------|------------------|------|-------|----------|
| | | | | | | | | | I-Shaped Damper | | | |
| | | | | | | | | | F_u | K | V_s | Ω |
| I-0.25-5.54-N | 10 | | 0.25 | 5.54 | 484.8 | 1126.2 | 315.25 | 1.54 | | | | |
| I-0.18-2.58-N | 15 | | 0.18 | 2.58 | 583.9 | 1254.7 | 350.48 | 1.67 | | | | |
| I-0.13-1.51-N | 20 | | 0.13 | 1.51 | 728 | 1438 | 400.11 | 1.82 | | | | |
| I-0.11-1.01-N | 25 | | 0.11 | 1.01 | 917 | 1684 | 469.75 | 1.95 | | | | |
| I-0.09-0.73-N | 30 | | 0.09 | 0.73 | 1155 | 1989 | 556.27 | 2.08 | | | | |
| X-0.25-5.54-1.21 | 10 | 2.5 | 0.25 | 5.54 | 748.60 | 1803.44 | 549.61 | 1.36 | 1.54 | 1.60 | 1.74 | 0.89 |
| X-0.25-5.54-0.60 | 10 | 5 | 0.25 | 5.54 | 1100.05 | 2405.06 | 673.29 | 1.63 | 2.27 | 2.14 | 2.14 | 1.06 |
| X-0.25-5.54-0.30 | 10 | 10 | 0.25 | 5.54 | 1958.83 | 3434.85 | 961.64 | 2.04 | 4.04 | 3.05 | 3.05 | 1.32 |
| X-0.25-5.54-0.15 | 10 | 20 | 0.25 | 5.54 | 3366.46 | 5047.38 | 1413.2 | 2.38 | 6.94 | 4.48 | 4.48 | 1.55 |
| X-0.18-2.58-1.21 | 15 | 2.5 | 0.18 | 2.58 | 815.29 | 1928.81 | 539.95 | 1.51 | 1.40 | 1.54 | 1.54 | 0.91 |
| X-0.18-2.58-0.60 | 15 | 5 | 0.18 | 2.58 | 1207.04 | 2532.93 | 709.09 | 1.7 | 2.07 | 2.02 | 2.02 | 1.02 |
| X-0.18-2.58-0.30 | 15 | 10 | 0.18 | 2.58 | 2107.93 | 3572.84 | 1000.3 | 2.11 | 3.61 | 2.85 | 2.85 | 1.26 |
| X-0.18-2.58-0.15 | 15 | 20 | 0.18 | 2.58 | 3531.51 | 5209.52 | 1458.6 | 2.42 | 6.05 | 4.15 | 4.16 | 1.45 |
| X-0.13-1.51-1.21 | 20 | 2.5 | 0.13 | 1.51 | 961.15 | 2099.45 | 587.72 | 1.64 | 1.32 | 1.46 | 1.47 | 0.90 |
| X-0.13-1.51-0.60 | 20 | 5 | 0.13 | 1.51 | 1376.29 | 2696.73 | 754.96 | 1.82 | 1.89 | 1.88 | 1.89 | 1.00 |
| X-0.13-1.51-0.30 | 20 | 10 | 0.13 | 1.51 | 2252.87 | 3730.70 | 1044.5 | 2.16 | 3.10 | 2.60 | 2.61 | 1.19 |
| X-0.13-1.51-0.15 | 20 | 20 | 0.13 | 1.51 | 3665.94 | 5368.18 | 1503 | 2.44 | 5.04 | 3.73 | 3.76 | 1.34 |
| X-0.11-1.01-1.21 | 25 | 2.5 | 0.11 | 1.01 | 1136.27 | 2325.69 | 651.07 | 1.75 | 1.24 | 1.38 | 1.39 | 0.89 |
| X-0.11-1.01-0.60 | 25 | 5 | 0.11 | 1.01 | 1575.04 | 2908.92 | 814.38 | 1.93 | 1.72 | 1.73 | 1.73 | 0.99 |
| X-0.11-1.01-0.30 | 25 | 10 | 0.11 | 1.01 | 2448.17 | 3924.41 | 1098.7 | 2.23 | 2.67 | 2.33 | 2.34 | 1.14 |
| X-0.11-1.01-0.15 | 25 | 20 | 0.11 | 1.01 | 3835.65 | 5544.21 | 1552.3 | 2.47 | 4.18 | 3.29 | 3.30 | 1.27 |
| X-0.09-0.73-1.21 | 30 | 2.5 | 0.09 | 0.73 | 1370.11 | 2604.33 | 665.22 | 1.9 | 1.19 | 1.31 | 1.20 | 0.91 |
| X-0.09-0.73-0.60 | 30 | 5 | 0.09 | 0.73 | 1822.76 | 3167.79 | 886.87 | 2.06 | 1.58 | 1.59 | 1.59 | 0.99 |
| X-0.09-0.73-0.30 | 30 | 10 | 0.09 | 0.73 | 2692.03 | 4155.37 | 1163.4 | 2.31 | 2.33 | 2.09 | 2.09 | 1.11 |
| X-0.09-0.73-0.15 | 30 | 20 | 0.09 | 0.73 | 4039.66 | 5743.36 | 1608.1 | 2.51 | 3.50 | 2.89 | 2.89 | 1.21 |

**Figure 5.** Comparing results of dampers with and without X-stiffeners (for dampers with $\rho = 0.25$ and $\rho = 0.09$).

6.2. Effect of ρ

To evaluate the effect of ρ on the performance of the dampers, the results are listed based on ρ in Table 3. Comparing the results indicates that although the reduction of ρ improves the results of both types of dampers, the I-shaped damper is more sensitive than the stiffened damper with X-stiffeners. When ρ is reduced from 0.25 to 0.09 (2.7 times), the F_u of the I-shaped dampers is improved by 1.2–2.38 times, whereas it is between 1.05 and 1.66 times for the stiffened dampers with X-stiffeners. Among the obtained results, ρ has the largest effect, respectively, on F_u , K , V_s , and Ω for the I-shaped dampers. However, for the stiffened dampers, ρ has the largest effect, respectively, on V_s , F_u , K , and Ω .

Table 3. Listed F_u , K , V_s , and Ω based on ρ .

| Model | ρ | F_u (kN) | K (kN/mm) | V_s (kN) | Ω | Damper with $\rho = i$ ($i = 0.18, 0.13, 0.11$, and 0.09) Divided by Damper with $\rho = 0.25$ | | | |
|------------------|--------|------------|-------------|------------|----------|---|------|-------|----------|
| | | | | | | F_u | K | V_s | Ω |
| I-0.25-5.54-N | 0.25 | 484.76 | 1126.24 | 315.25 | 1.54 | | | | |
| I-0.18-2.58-N | 0.18 | 583.88 | 1254.71 | 350.48 | 1.67 | 1.2 | 1.11 | 1.11 | 1.08 |
| I-0.13-1.51-N | 0.13 | 727.55 | 1437.6 | 400.11 | 1.82 | 1.5 | 1.28 | 1.27 | 1.18 |
| I-0.11-1.01-N | 0.11 | 917.02 | 1684.32 | 469.75 | 1.95 | 1.89 | 1.50 | 1.49 | 1.27 |
| I-0.09-0.73-N | 0.09 | 1155.3 | 1989.45 | 556.27 | 2.08 | 2.38 | 1.77 | 1.76 | 1.35 |
| X-0.25-5.54-1.21 | 0.25 | 748.6 | 1803.44 | 315.25 | 1.54 | | | | |
| X-0.25-5.54-0.60 | 0.18 | 815.29 | 1928.81 | 556.27 | 2.08 | 1.09 | 1.07 | 1.76 | 1.35 |
| X-0.25-5.54-0.30 | 0.13 | 961.15 | 2099.45 | 1413.17 | 2.38 | 1.28 | 1.16 | 4.48 | 1.55 |
| X-0.25-5.54-0.15 | 0.11 | 1136.3 | 2325.69 | 1458.58 | 2.42 | 1.52 | 1.29 | 4.63 | 1.57 |
| X-0.18-2.58-1.21 | 0.09 | 1370.1 | 2604.33 | 1503.03 | 2.44 | 1.83 | 1.44 | 4.77 | 1.59 |
| X-0.18-2.58-0.60 | 0.25 | 1100.1 | 2405.06 | 350.48 | 1.67 | | | | |
| X-0.18-2.58-0.30 | 0.18 | 1207 | 2532.93 | 549.61 | 1.36 | 1.10 | 1.05 | 1.57 | 0.82 |
| X-0.18-2.58-0.15 | 0.13 | 1376.3 | 2696.73 | 539.95 | 1.51 | 1.25 | 1.12 | 1.54 | 0.91 |
| X-0.13-1.51-1.21 | 0.11 | 1575 | 2908.92 | 587.72 | 1.64 | 1.43 | 1.21 | 1.68 | 0.98 |
| X-0.13-1.51-0.60 | 0.09 | 1822.8 | 3167.79 | 651.07 | 1.75 | 1.66 | 1.32 | 1.86 | 1.05 |
| X-0.13-1.51-0.30 | 0.25 | 1958.8 | 3434.85 | 400.11 | 1.82 | | | | |
| X-0.13-1.51-0.15 | 0.18 | 2107.9 | 3572.84 | 673.29 | 1.63 | 1.08 | 1.04 | 1.68 | 0.9 |
| X-0.11-1.01-1.21 | 0.13 | 2252.9 | 3730.7 | 709.09 | 1.7 | 1.15 | 1.09 | 1.77 | 0.94 |
| X-0.11-1.01-0.60 | 0.11 | 2448.2 | 3924.41 | 754.96 | 1.82 | 1.25 | 1.14 | 1.89 | 1 |
| X-0.11-1.01-0.30 | 0.09 | 2692 | 4155.37 | 814.38 | 1.93 | 1.37 | 1.21 | 2.04 | 1.06 |
| X-0.11-1.01-0.15 | 0.25 | 3366.5 | 5047.38 | 469.75 | 1.95 | | | | |
| X-0.09-0.73-1.21 | 0.18 | 3531.5 | 5209.52 | 961.64 | 2.04 | 1.05 | 1.03 | 2.05 | 1.04 |
| X-0.09-0.73-0.60 | 0.13 | 3665.9 | 5368.18 | 1000.28 | 2.11 | 1.09 | 1.06 | 2.13 | 1.08 |
| X-0.09-0.73-0.30 | 0.11 | 3835.7 | 5544.21 | 1044.49 | 2.16 | 1.14 | 1.1 | 2.22 | 1.1 |
| X-0.09-0.73-0.15 | 0.09 | 4039.7 | 5743.36 | 1098.74 | 2.23 | 1.20 | 1.14 | 2.34 | 1.14 |

6.3. Effect of β'

While developing the relationship to predict the behavior of the proposed dampers, it was revealed that β' improves the performance of the dampers. This issue is confirmed by the plots in Figure 6 regarding the comparison of the load-rotation graphs of the dampers.

Figure 7 displays the impact of β' on F_u , K , V_s , and Ω . As shown in this figure, increasing β' enhances the mentioned parameters, but the rate of the enhancement for each parameter is different. F_u and K have the same improvement related to β' . Similar enhancement related to β' is also observed for V_s and Ω . According to the figure, β' has an approximately linear relation with F_u , K , and V_s , which is confirmed by $K = nK_p \left(1 + \frac{\Delta_p}{\Delta_f} \beta + \frac{\Delta_p}{\Delta_s} \beta'\right)$ and $V_n = nV_p(1 + \beta + \beta')$. However, β' has nonlinear relation with Ω because it has emerged in the denominator of $\Omega = \frac{1 + \psi' + \psi}{1 + K_f \frac{\beta}{\beta'} + K_s \frac{\beta'}{\beta}}$. Since β completely changes ρ , F_u and K are sensitive to ρ . For a primary design, F_u and K are proposed as:

$$F_u = 82 \left(\frac{0.25}{\rho} \right)^2 \beta' + \frac{96}{\rho} \quad (17)$$

$$K = 110 \left(\frac{0.25}{\rho} \right)^2 \beta' + \frac{365}{\rho} \quad (18)$$

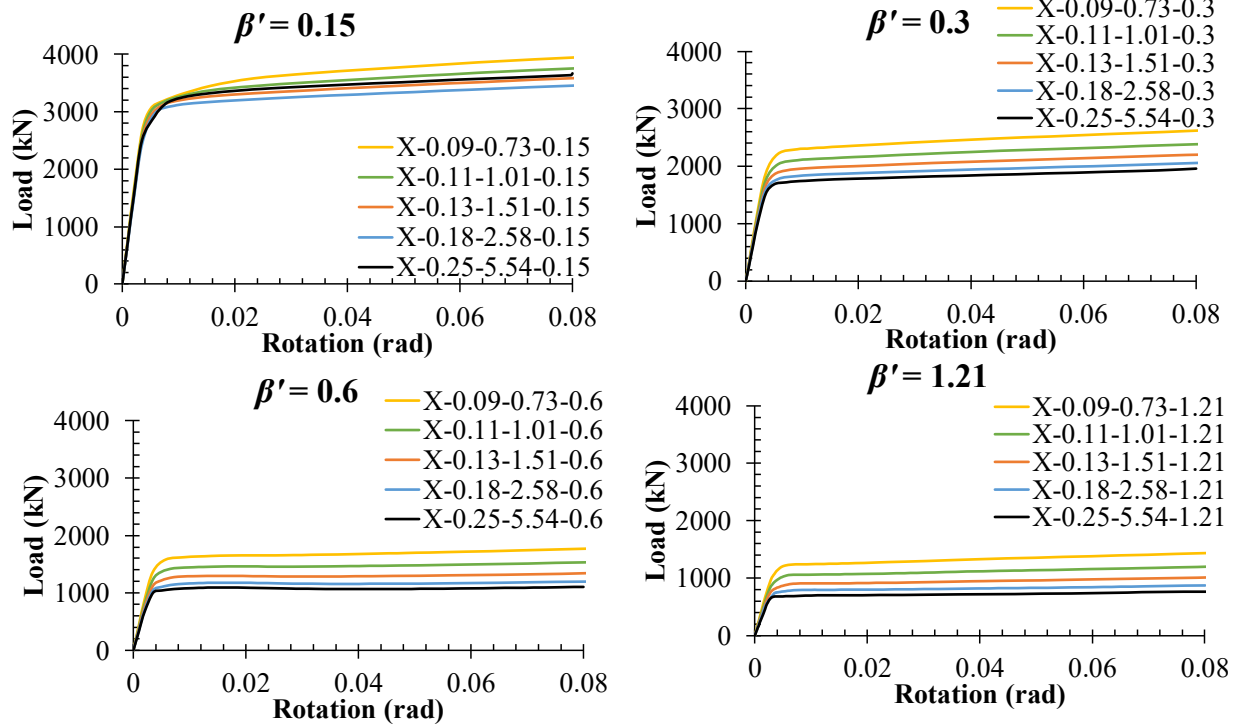


Figure 6. Comparing load-rotation graphs of dampers based on β' .

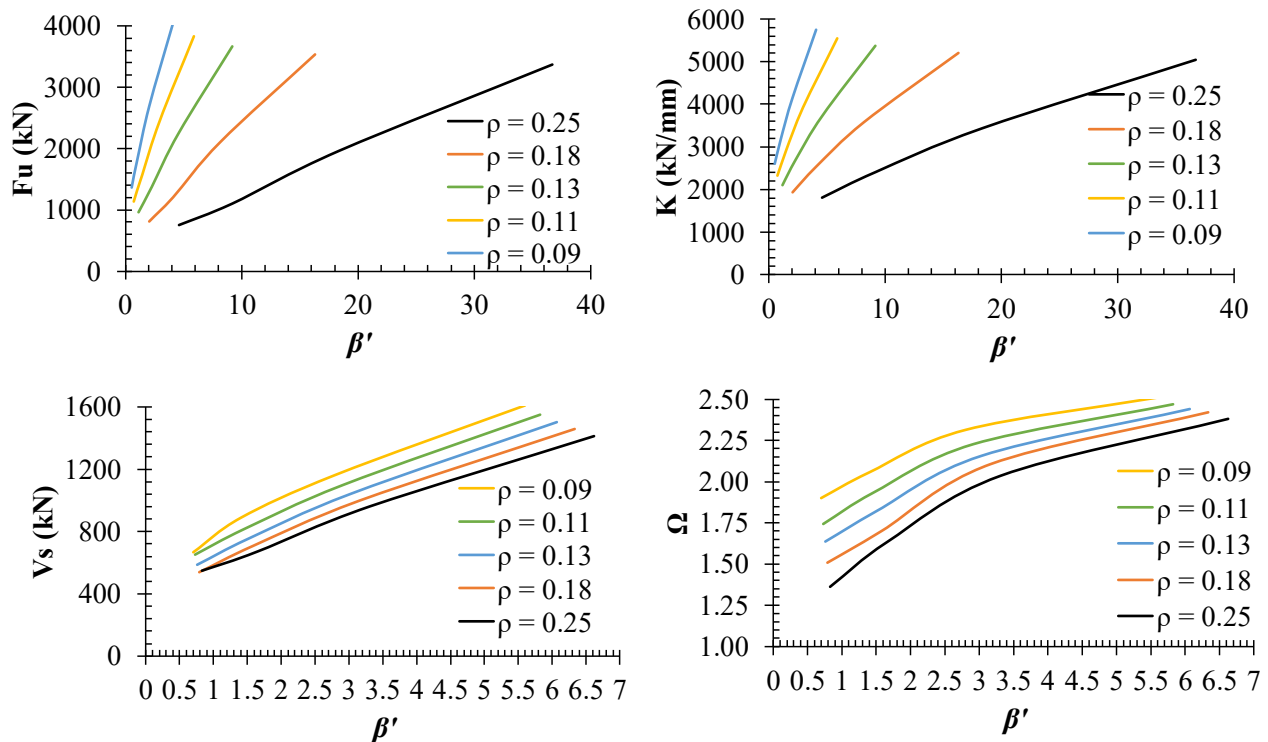


Figure 7. F_u , K , V_s , and Ω versus β' .

6.4. Effect of L_s/t_s and b_s/t_s

In Figure 8, the structural performance (F_u , K , V_s , and Ω) are drawn versus slenderness ratio (L_s/t_s) and b_s/t_s . As expected, by the reduction of the mentioned ratios, F_u , K , V_s , and Ω are improved. This figure indicates that F_u , V_s , and K are affected by L_s/t_s and b_s/t_s . The dependence of the parameters on L_s/t_s can be categorized into three parts: $L_s/t_s < 18$, $20 < L_s/t_s < 30$, and $L_s/t_s > 30$. In the first part, the maximum reduction occurs, the rate of reduction dwindles in the second part, and the third part shows a smooth reduction. Since in the first and second parts, F_u is very sensitively dependent on L_s/t_s , the range of $30 < L_s/t_s < 80$ is proposed for the design of the stiffeners. As similar performance is seen for b_s/t_s in three parts of $b_s/t_s < 15$, $15 < b_s/t_s < 30$, and $b_s/t_s > 30$, then $30 < b_s/t_s < 60$ is recommended.

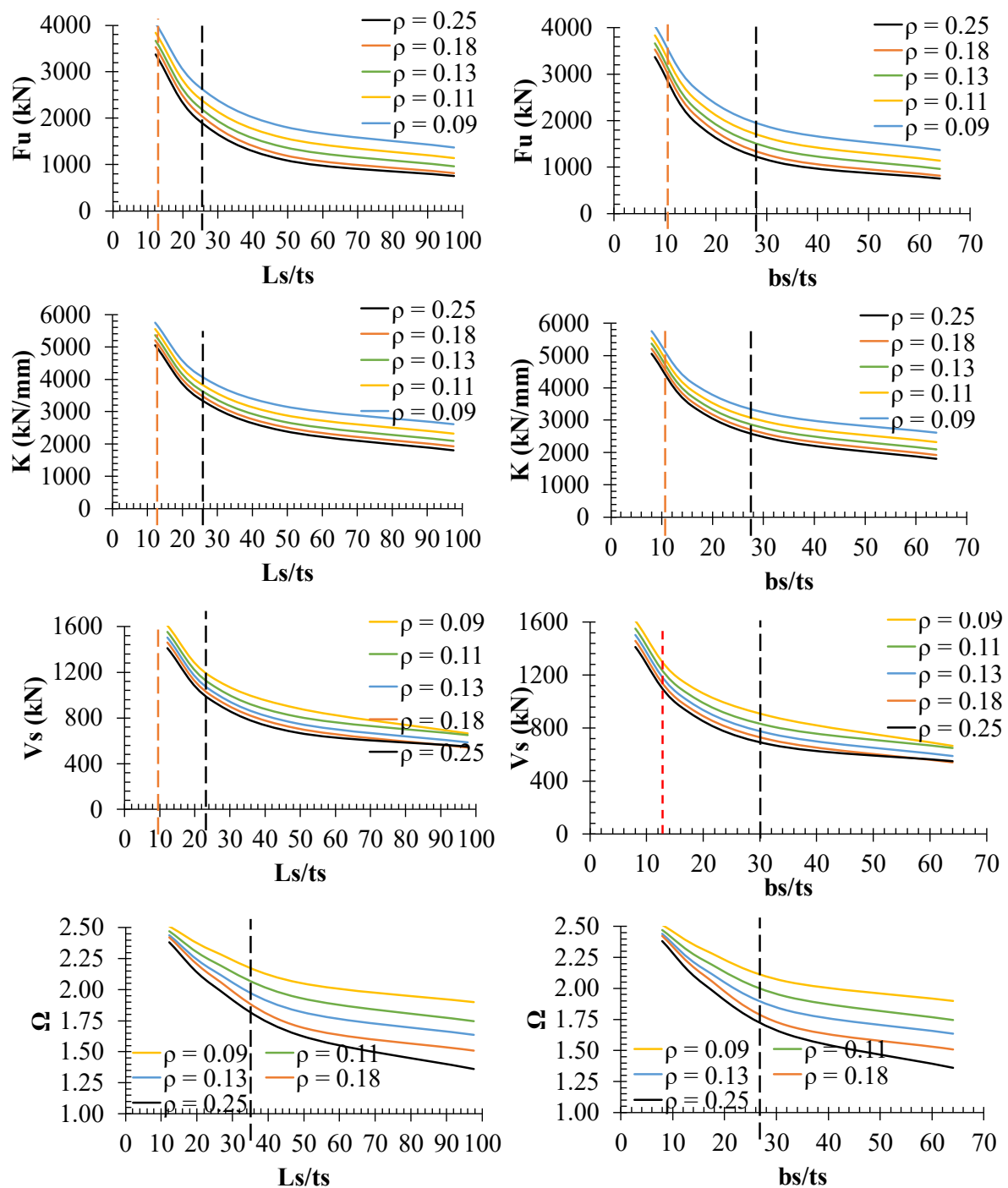


Figure 8. F_u , K , V_s , and Ω versus L_s/t_s and b_s/t_s .

Ω is also affected by L_s/t_s , b_s/t_s , and ρ . For small L_s/t_s and b_s/t_s , the effect of ρ on Ω is ignorable, and it is recommended to have $\Omega = 2.5$ in the design of elements outside the damper. However, for L_s/t_s lower or greater than 40 and for b_s/t_s lower or larger than 30, the rate of reduction in Ω is changed, which is related to ρ . Consequently, for achieving a high value of Ω , L_s/t_s and b_s/t_s should be greater than 40 and 30, respectively.

6.5. Effect of t_s/t_f and t_s/t_p

In addition to knowing the effect of t_s/t_f and t_s/t_p on the performance of the damper, selecting an appropriate ratio is important in the primary design. The proper ratio of t_s/t_f and t_s/t_p in the primary design not only reduces the trial and error to achieve the optimal design but also guarantees the suitable performance of the damper. Accordingly, F_u , K , V_s , and Ω are plotted versus t_s/t_f and t_s/t_p in Figure 9. It can be concluded from the figure that increasing either t_s/t_f (β'/β) or t_s/t_p improves the performance of the dampers. The noticeable issue is that this improvement with the increase in t_s/t_p is inconsiderably affected by ρ , while the increase in t_s/t_f is significantly affected by ρ . Therefore, it can be stated that increasing the t_s/t_p directly increases F_u , K , V_s , and Ω . To achieve a better F_u and K , this figure indicates that t_s/t_p should be larger than 1, while for Ω it is recommended to have $t_s/t_p > 1.5$. However, with $t_s/t_f > 1$, a suitable result is obtained.

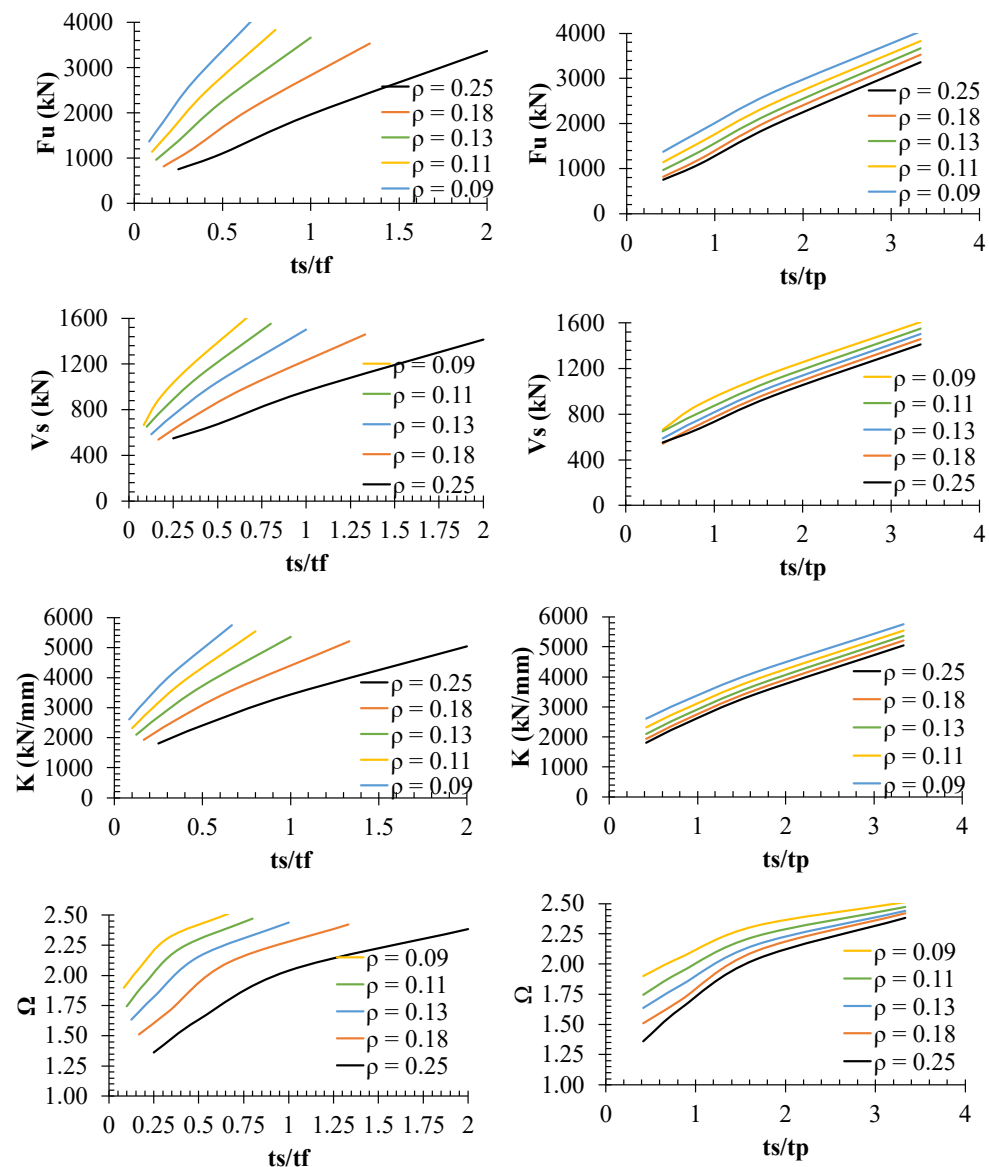


Figure 9. Effect of t_s/t_f and t_s/t_p on F_u , V_s , K , and Ω .

6.6. Accuracy of Proposed Equations

To assure the accuracy of the proposed equations in predicting the structural performance (F_u , K , V_s , and Ω) of the proposed damper, the outcomes from the proposed equations are compared with the FE results in Table 4. The comparison demonstrates a good agreement between the results from the proposed equations and the FE, which illustrates the acceptable accuracy of the proposed equations.

Table 4. Comparing results from proposed equations with FE.

| Models | FE | | | Proposed Equations | | | FE/Proposed Equations | | |
|------------------|------------|-------------|----------|--------------------|-------------|----------|-----------------------|-------------|----------|
| | F_u (kN) | K (kN/mm) | Ω | F_u (kN) | K (kN/mm) | Ω | F_u (kN) | K (kN/mm) | Ω |
| I-0.25-5.54-N | 484.76 | 1126.24 | 1.54 | 400.46 | 719.15 | 1.42 | 0.93 | 1.57 | 0.93 |
| I-0.18-2.58-N | 583.88 | 1254.71 | 1.67 | 469.03 | 887.67 | 1.57 | 0.94 | 1.41 | 0.94 |
| I-0.13-1.51-N | 727.55 | 1437.60 | 1.82 | 565.03 | 1187.39 | 1.72 | 0.95 | 1.21 | 0.95 |
| I-0.11-1.01-N | 917.02 | 1684.32 | 1.95 | 688.46 | 1662.03 | 1.83 | 0.94 | 1.01 | 0.94 |
| I-0.09-0.73-N | 1155.30 | 1989.45 | 2.08 | 839.31 | 2355.34 | 1.92 | 0.92 | 0.84 | 0.92 |
| X-0.25-5.54-1.21 | 748.60 | 1803.44 | 1.36 | 715.04 | 1378.93 | 1.39 | 1.02 | 1.31 | 1.02 |
| X-0.25-5.54-0.60 | 1100.05 | 2405.06 | 1.63 | 1029.63 | 2038.72 | 1.60 | 0.98 | 1.18 | 0.98 |
| X-0.25-5.54-0.30 | 1958.83 | 3434.85 | 2.04 | 1658.80 | 3358.28 | 1.78 | 0.87 | 1.02 | 0.87 |
| X-0.25-5.54-0.15 | 3366.46 | 5047.38 | 2.38 | 2917.14 | 5997.42 | 2.10 | 0.88 | 0.84 | 0.88 |
| X-0.18-2.58-1.21 | 815.29 | 1928.81 | 1.51 | 783.61 | 1547.45 | 1.60 | 1.06 | 1.25 | 1.06 |
| X-0.18-2.58-0.60 | 1207.04 | 2532.93 | 1.70 | 1098.20 | 2207.24 | 1.67 | 0.98 | 1.15 | 0.98 |
| X-0.18-2.58-0.30 | 2107.93 | 3572.84 | 2.11 | 1727.37 | 3526.81 | 1.81 | 0.86 | 1.01 | 0.86 |
| X-0.18-2.58-0.15 | 3531.51 | 5209.52 | 2.42 | 2985.71 | 6165.94 | 2.10 | 0.87 | 0.84 | 0.87 |
| X-0.13-1.51-1.21 | 961.15 | 2099.45 | 1.64 | 879.61 | 1847.17 | 1.71 | 1.04 | 1.14 | 1.04 |
| X-0.13-1.51-0.60 | 1376.29 | 2696.73 | 1.82 | 1194.20 | 2506.96 | 1.75 | 0.96 | 1.08 | 0.96 |
| X-0.13-1.51-0.30 | 2252.87 | 3730.70 | 2.16 | 1823.37 | 3826.52 | 1.86 | 0.86 | 0.97 | 0.86 |
| X-0.13-1.51-0.15 | 3665.94 | 5368.18 | 2.44 | 3081.71 | 6465.66 | 2.13 | 0.87 | 0.83 | 0.87 |
| X-0.11-1.01-1.21 | 1136.27 | 2325.69 | 1.75 | 1003.04 | 2321.82 | 1.80 | 1.03 | 1.00 | 1.03 |
| X-0.11-1.01-0.60 | 1575.04 | 2908.92 | 1.93 | 1317.63 | 2981.60 | 1.83 | 0.95 | 0.98 | 0.95 |
| X-0.11-1.01-0.30 | 2448.17 | 3924.41 | 2.23 | 1946.80 | 4301.17 | 1.93 | 0.87 | 0.91 | 0.87 |
| X-0.11-1.01-0.15 | 3835.65 | 5544.21 | 2.47 | 3205.14 | 6940.31 | 2.18 | 0.88 | 0.80 | 0.88 |
| X-0.09-0.73-1.21 | 1370.11 | 2604.33 | 1.90 | 1153.90 | 3015.12 | 2.08 | 1.01 | 0.86 | 1.09 |
| X-0.09-0.73-0.60 | 1822.76 | 3167.79 | 2.06 | 1468.48 | 3674.90 | 1.91 | 0.93 | 0.86 | 0.93 |
| X-0.09-0.73-0.30 | 2692.03 | 4155.37 | 2.31 | 2097.65 | 4994.47 | 2.00 | 0.86 | 0.83 | 0.86 |
| X-0.09-0.73-0.15 | 4039.66 | 5743.36 | 2.51 | 3355.99 | 7633.61 | 2.23 | 0.89 | 0.75 | 0.89 |

7. Conclusions

An innovative damper was introduced and investigated numerically and parametrically in this article. In addition, required equations were suggested for the design and prediction of the performance of the system. Results indicated that the suggested equations are in good agreement with the FE results. Moreover, the findings are summarized as follows:

- Adding the X-stiffeners to the I-shaped dampers improves their performance.
- Low t_s increases F_u between 19 and 54%, whereas it can reach 3.5–6.94 times by thick stiffeners. Additionally, the elastic stiffness is enhanced by the thin and thick stiffeners, respectively, between 31–60% and 2.89–4.48 times.
- By adding the thin stiffeners, Ω is reduced around 10%, whereas by increasing t_s , it is improved between 21 and 55%.
- Although ρ affects the response curve of the dampers, F_u and the elastic stiffness do not have an impact on the stiffness in the nonlinear zone.
- For $\psi' < 1$ or $V_p < V_s$, the largest reduction of F_u and K occurred. However, in $\psi' > 1$ or $V_p > V_s$, the reduction tends to coincide with different values of ρ . Therefore, when $\psi' < 1$ or $V_p < V_s$, F_u and K are considerably sensitive to ρ .

- Considering the behavior of the dampers, it was indicated that better performance of the damper is obtained when $V_s > V_f$.
- The dependence of the parameters; F_u , K , V_s , and Ω on L_s/t_s can be categorized into three parts: $L_s/t_s < 18$, $20 < L_s/t_s < 30$, and $L_s/t_s > 30$. In the first part, the maximum reduction occurs, the rate of reduction dwindles in the second part, and the third part shows a smooth reduction.
- Since for $L_s/t_s < 18$ and $20 < L_s/t_s < 30$, F_u is very sensitively dependent on L_s/t_s , the range of $30 < L_s/t_s < 80$ is proposed for the design of the stiffeners. A similar performance is seen for b_s/t_s in $b_s/t_s < 15$, $15 < b_s/t_s < 30$, and $b_s/t_s > 30$, then $30 < b_s/t_s < 60$ is recommended.
- For small L_s/t_s and b_s/t_s , the effect of ρ on Ω is ignorable, and it is recommended to have $\Omega = 2.5$ in the design of the elements outside the damper. However, for L_s/t_s lower or greater than 40 and for b_s/t_s lower or larger than 30, the reduction rate of Ω is changed, which is related to ρ .

8. Recommendations for Future Works

It is recommended to investigate the strengthening of the reinforced concrete (RC) with the proposed damper. It is expected that the proposed damper shows a suitable performance for strengthening the RC frames. However, it is necessary to compare it with other conventional systems for reinforcing the RC frames. A comprehensive study is required to evaluate the interaction between the damper and RC frame, the connection of the damper to the RC frame, and achieving the effective structural parameters.

Author Contributions: Conceptualization, A.G.; methodology, A.B., A.G. and O.B.; validation, A.B., A.G., C.T. and O.B.; investigation, A.B., A.G., C.T. and O.B.; resources, A.B., A.G., C.T. and O.B.; writing—original draft preparation, A.B., A.G., C.T. and O.B.; writing—review and editing, A.B. All authors have read and agreed to the published version of the manuscript.

Funding: This research received no external funding.

Data Availability Statement: Not applicable.

Conflicts of Interest: The authors declare no conflict of interest.

References

1. Zhao, Z.; Zhang, W.; Ding, Y.; Li, H. Effects of Reserve Capacity on Seismic Response of Concentrically Braced Frames by Considering Brace Failure. *Materials* **2022**, *15*, 4377. [\[CrossRef\]](#) [\[PubMed\]](#)
2. Bagheri, A.; Hadidi, A.; Alilou, A. Heightwise Distribution of Stiffness Ratio for Optimum Seismic Design of Steel Frames with Metallic-Yielding. *Procedia Eng.* **2011**, *14*, 2891–2898. [\[CrossRef\]](#)
3. Khavari, M. Investigation on Dynamics Nonlinear Analysis of Steel Frames with Steel Dampers. *Procedia Eng.* **2013**, *54*, 401–412. [\[CrossRef\]](#)
4. Chen, Y.; Yu, W.; Zhang, M.; Li, Y. A novel energy dissipation damper for multi-level earthquakes. *J. Constr. Steel Res.* **2022**, *192*, 107214. [\[CrossRef\]](#)
5. Xu, Y.; Xu, Z.; Guo, Y.; Huang, X.; Dong, Y.; Li, Q. Dynamic Properties and Energy Dissipation Study of Sandwich Viscoelastic Damper Considering Temperature Influence. *Buildings* **2021**, *11*, 470. [\[CrossRef\]](#)
6. Chalarca, B.; Filiatrault, A.; Perrone, D. Parametric study and prediction models of the seismic response of single-degree-of-freedom structural systems equipped with Maxwell material fluid viscous dampers. *Structures* **2022**, *43*, 388–406. [\[CrossRef\]](#)
7. Dong, B.; Ricles, J. Simplified seismic design procedure for steel MRF structure with nonlinear viscous dampers. *J. Constr. Steel Res.* **2021**, *185*, 106857. [\[CrossRef\]](#)
8. Ramhormozian, S.; Clifton, G.C.; Latour, M.; MacRae, G.A. Proposed Simplified Approach for the Seismic Analysis of Multi-Storey Moment Resisting Framed Buildings Incorporating Friction Sliders. *Buildings* **2019**, *9*, 130. [\[CrossRef\]](#)
9. Guo, J.; Li, H.; Zhang, C.; Chu, S.; Dang, X. Effect of an Innovative Friction Damper on Seismic Responses of a Continuous Girder Bridge under Near-Fault Excitations. *Buildings* **2022**, *12*, 1019. [\[CrossRef\]](#)
10. Ramhormozian, S.; Clifton, G.C.; MacRae, G.A.; Davet, G.P. Stiffness-based approach for Belleville springs use in friction sliding structural connections. *J. Constr. Steel Res.* **2017**, *138*, 340–356. [\[CrossRef\]](#)
11. Zhou, X.; Sun, T.; Sun, B.; Ma, N.; Ou, J. Vibration-Reduction Strategy for High-Rise Braced Frame Using Viscoelastic-Yielding Compounded BRB. *Buildings* **2022**, *12*, 1159. [\[CrossRef\]](#)
12. Wang, J.; Lu, F.; Li, F. Subassembly tests and analysis of buckling-restrained braced reinforced concrete frames with various gusset connections. *Structures* **2022**, *39*, 39–56. [\[CrossRef\]](#)

13. Bai, J.; Chen, H.; Ma, G.; Duan, L. Development of a four-tube-assembled buckling-restrained brace for convenient post-earthquake damage examination and replacement. *J. Build. Eng.* **2022**, *50*, 104209. [\[CrossRef\]](#)
14. Castaldo, P.; Tubaldi, E.; Selvi, F.; Gioiella, L. Seismic performance of an existing RC structure retrofitted with buckling restrained braces. *J. Build. Eng.* **2021**, *33*, 101688. [\[CrossRef\]](#)
15. Zhao, B.; Lu, B.; Zeng, X.; Gu, Q. Experimental and numerical study of hysteretic performance of new brace type damper. *J. Constr. Steel Res.* **2021**, *183*, 106717. [\[CrossRef\]](#)
16. Tsai, K.-C. Design of steel triangular plate energy absorbers for seismic-resistant construction. *Earthq. Spectra* **1993**, *9*, 505–528. [\[CrossRef\]](#)
17. Liyanage, U.D.D.; Perera, T.N.; Maneetes, H. Analysis of X-shaped and Double X-shaped Metallic Dampers on Multistorey Frames. *J. Univ. Ruhuna* **2020**, *7*, 12–24. [\[CrossRef\]](#)
18. Bergman, D.M.; Goel, S.C. *Evaluation of Cyclic Testing of Steel-Plate Devices for Added Damping and Stiffness*; Department of Civil Engineering, University of Michigan: Ann Arbor, MI, USA, 1987.
19. Xia, C.; Hanson, R.D. Influence of ADAS Element Parameters on Building Seismic, Response. *J. Struct. Eng.* **1992**, *118*, 1903–1918. [\[CrossRef\]](#)
20. Askariani, S.; Garivani, S. Introducing and numerical study of a new brace-type slit damper. *Structures* **2020**, *27*, 702–717. [\[CrossRef\]](#)
21. Lu, L.; Xu, Y.; Liu, J.; Lim, J. Cyclic performance and design recommendations of a novel weak-axis Reduced Beam Section connection. *Steel Compos. Struct.* **2018**, *27*, 1–12.
22. Rai, D.; Benjamin, J. Aluminium shear-links for enhanced seismic resistance. *Earthq. Eng. Struct. Dyn.* **1998**, *27*, 315–342. [\[CrossRef\]](#)
23. Ghamari, A.; Kim, C.; Jeong, S.H. Development of an innovative metallic damper for concentrically braced frame systems based on experimental and analytical studies. *Struct. Des. Tall Spec. Build.* **2022**, *31*, e1927. [\[CrossRef\]](#)
24. Ghamari, A.; Almasi, B.; Kim, C.-h.; Jeong, S.H.; Hong, K.-J. An Innovative Steel Damper with a Flexural and Shear-Flexural Mechanism to Enhance the CBF System Behavior: An Experimental and Numerical Study. *Appl. Sci.* **2021**, *11*, 11454. [\[CrossRef\]](#)
25. Ghamari, A.; Haeri, H.; Khaloo, A.; Zhu, Z. Improving the hysteretic behavior of Concentrically Braced Frame (CBF) by a proposed shear damper. *Steel Compos. Struct.* **2019**, *30*, 383–392. [\[CrossRef\]](#)
26. Thongchom, C.; Mirzai, N.; Chang, B.; Ghamari, A. Improving the CBF brace's behavior using I-shaped dampers, numerical and experimental study. *J. Constr. Steel Res.* **2022**, *197*, 107482. [\[CrossRef\]](#)
27. Hjelmstad, K.D.; Popov, E.P. *Seismic Behavior of Active Beam Link in Eccentrically Braced Frames*; Rep. No. UCB/EERC-83/15; Earthquake Engineering Research Center, University of California: Berkeley, CA, USA, 1983.
28. Kasai, K.; Popov, E.P. *A Study of Seismically Resistant Eccentrically Braced 418 Frames*; Rep. No. UCB/EERC-86/01; Earthquake Engineering Research Center, University of California: Berkeley, CA, USA, 1986.
29. Popov, E.P.; Engelhardt, M.D. Seismic eccentrically braced frames. *J. Constr. Steel Res.* **1988**, *10*, 321–354. [\[CrossRef\]](#)
30. Okazaki, T.; Arce, G.; Ryu, H.C.; Engelhardt, M.D. Experimental study of 431 local buckling, overstrength, and fracture of links in eccentrically braced frames. *J. Struct.* **2005**, *131*, 1526–1535.433.
31. Bahrami, A.; Heidari, M. Investigation of steel frames equipped with steel eccentric braces and steel-concrete buckling restrained braces having moment link. *Open Construct. Build. Technol. J.* **2021**, *15*, 55–69. [\[CrossRef\]](#)
32. Bahrami, A.; Heidari, M. Evaluation of structural response of composite steel-concrete eccentrically buckling-restrained braced frames. *J. Appl. Eng. Sci.* **2020**, *18*, 591–600. [\[CrossRef\]](#)
33. Seki, M.; Katsumata, H.; Uchida, H.; Takeda, T. Study on earthquake response of two-storied steel frame with Y-shaped braces. In Proceedings of the 9th World Conference on Earthquake Engineering, Tokyo-Kyoto, Japan, 7–9 August 1998; pp. 65–70.
34. Baradaran, M.R.; Hamzezarghani, F.; RastegariGhiri, M.; Mirsanjari, Z. The effect of vertical shear-link in improving the seismic performance of structures with eccentrically bracing systems. *Int. J. Civil. Environ. Eng.* **2015**, *9*, 1078–1082.
35. Vetr, M.; Ghamari, A. Experimentally and analytically study on eccentrically braced frame with vertical shear links. *Struct. Des. Tall Spec. Build.* **2019**, *28*, e1587. [\[CrossRef\]](#)
36. Bouwkamp, J.; Vetr, M.; Ghamari, A. An analytical model for inelastic cyclic response of eccentrically braced frame with vertical shear link (V-EBF). *Case Stud. Struct. Eng.* **2016**, *6*, 31–44. [\[CrossRef\]](#)
37. Caprili, S.; Morelli, F.; Mussini, N. Walter SALVATORE, Experimental tests on real-scale EBF structures with horizontal and vertical links. *Data Brief* **2018**, *21*, 1246–1257. [\[CrossRef\]](#)
38. ANSI/AISC 360-16, Specification for Structural Steel Buildings. *Inst. Steel Constr. Am.* **2016**, *1*, 1–612.
39. McDaniel, C.; Uang, C.; Seible, F. Cyclic testing of built-up steel shear links for the new bay bridge. *J. Struct. Eng. ASCE* **2003**, *129*, 801–809. [\[CrossRef\]](#)
40. Manheim, D.N.; Popov, E.P. Plastic shear hinges in steel frames. *J. Struct. Eng. ASCE* **1983**, *109*, 2404–2419. [\[CrossRef\]](#)
41. Richards, P.W. Cyclic Stability and Capacity Design of Steel Eccentrically Braced Frames. Ph.D. Thesis, Department of Structural Engineering, University of California, San Diego, CA, USA, 2004.
42. Ghamari, A.; Kim, Y.-J.; Bae, J. An Innovative shear link as damper: An experimental and numerical study. *Steel Compos. Struct.* **2022**, *42*, 539–552. [\[CrossRef\]](#)